文章编号: 1000-0887(2007) 12-1411-06

压电弯曲元的夹层梁解析模型*

周燕国, 陈云敏, 凌道盛 江

(浙江大学 软弱土与环境土工教育部重点实验室, 杭州 310027)

(我刊编委 凌道盛 江来稿)

摘要: 压电弯曲元是一类传感和作动器件, 已得到广泛的应用. 基于一阶剪切变形理论发展了压电弯曲元夹层梁解析模型, 对梁截面采用统一转角并将耦合电势沿厚度的分布假设为二次函数, 进一步修正了横向剪应变对电位移的影响. 以弯曲元简支梁自由振动为例进行数值分析, 解析模型解与二维精确解相比具有良好的精度, 为分析弯曲元动力机电响应提供了良好的解析模型.

关 键 词: 弯曲元; 压电; 夹层梁; 剪切系数; 解析模型

中图分类号: O343.1 文献标识码: A

引 言

压电弯曲元是一种机-电传感器, 能利用压电效应将机械能转换为电能, 反之亦然. 弯曲元最早由 Shirley 和 Hampton[1] 引入到岩土实验中, 作为剪切波的激发元和接收元, 通过测量试样中剪切波速进而计算土体小应变剪切模量. 经过几十年的发展, 弯曲元技术已成为岩土工程中土体剪切波速测量的有效手段[2-3]. 然而, 在应用过程中发现, 剪切波传播时间判定的主观性会带来显著误差, 一般认为, 这种判断误差源于对压电弯曲元的机电耦合振动特性和剪切波在土样中传播与衰减机理上的认识不够[4-5]. 因此, 对弯曲元机电耦合振动的研究成为当前研究的热点[6-7].

弯曲元通常由两层外表面镀有均匀电极的压电陶瓷层和中间导电金属层胶结而成, 是一种典型的对称压电夹层结构. 说际测试中, 弯曲元装配在仪器基座两端以悬臂梁形式进行波的激发和接收. 目前对此类压电悬臂梁结构无法直接获得精确解, 分析弯曲元振动需建立合理有效的简化模型[8-10]. 本文结合弯曲元压电层较厚的具体特征, 建立了基于一阶剪切变形理论的压电夹层梁解析模型. 弯曲元简支梁自由振动的计算分析表明, 与二维精确解相比, 本文压电夹层梁模型具有良好的精度.

1 基 本 方 程

在弯曲元中, 对于正交各向异性压电层, 假设在 x-z 坐标面的平面梁处于平面应力状态

* 收稿日期: 2007-04-16; 修订日期: 2007-10-28
基金项目: 国家自然科学基金资助项目(10472102); 国家 973 计划资助项目(2007CB714200)
作者简介: 周燕国(1978—), 男, 浙江富阳人, 博士;
陈云敏, 教授(联系人. Tel: +86-571-87951340; Fax: +86-571-87952165; E-mail: chenyunmin@zju.edu.cn).

($\sigma_y = \tau_{xy} = \tau_{yz} = 0, D_y = 0$), 从二维压电弹性力学基本方程[11] 出发, 进一步略去横向挤压应力($\sigma_z = 0$) 之后[12], 有如下基本方程(不考虑体积力):

$$\frac{\partial\sigma_x}{\partial x} + \frac{\partial\tau_{xz}}{\partial z} = \rho\frac{\partial^2 u_x}{\partial t^2},\quad \frac{\partial\tau_{xz}}{\partial x} = \rho\frac{\partial^2 u_z}{\partial t^2},\quad \frac{\partial D_x}{\partial x} + \frac{\partial D_z}{\partial z} = 0, \tag{1}$$

$$\sigma_x = c_{11}\varepsilon_x + (-1)^j e_{31}\frac{\partial\phi}{\partial z},\quad \tau_{xz} = c_{55}\gamma_{xz} + (-1)^j e_{15}\frac{\partial\phi}{\partial x}, \tag{2}$$

$$D_z = (-1)^j e_{31}\varepsilon_x - \varepsilon_{33}\frac{\partial\phi}{\partial z},\quad D_x = (-1)^j e_{15}\gamma_{xz} - \varepsilon_{11}\frac{\partial\phi}{\partial x}, \tag{3}$$

式中, σ_x、τ_{xz}、u_x、u_z、D_x、D_z 和 ϕ 分别代表应力、位移、电位移和电势分量; c_{11}、e_{31} 和 ε_{33} 分别是折算弹性模量、压电常数和介电常数, 分别为

$$\begin{cases} c_{11} = c_{11} - \dfrac{c_{12}^2}{c_{22}} - \dfrac{(c_{13}c_{22} - c_{12}c_{23})^2}{c_{22}(c_{22}c_{33} - c_{23}^2)},\quad \varepsilon_{33} = \varepsilon_{33} + \dfrac{e_{32}^2}{c_{22}} + \dfrac{(c_{22}e_{33} - c_{23}e_{32})^2}{c_{22}(c_{22}c_{33} - c_{23}^2)}, \\ e_{31} = e_{31} - \dfrac{c_{12}e_{32}}{c_{22}} - \dfrac{(c_{13}c_{22} - c_{12}c_{23})(c_{22}e_{33} - c_{23}e_{32})}{c_{22}(c_{22}c_{33} - c_{23}^2)}. \end{cases} \tag{4}$$

式(2) 和(3) 中的上标 j 指示压电层的极化方向, 极化方向与 z 轴一致或相反, 分别取 j 等于 2 或 1. 不失一般性, 假设上层极化方向总是与 z 轴正向一致.

对于弹性层, 上述方程可简化为 4 个方程, 保留式(1) 的前 2 式和式(2), 并令式(2) 中 $e_{31} = e_{15} = 0$. 对各向同性材料, $c_{11} = E$, $c_{55} = E/[2(1+\nu)]$, 其中 E 为弹性模量, ν 是 Poisson 比.

2 位移假设和内力计算

采用一阶剪切变形理论, 假设弯曲元各层有统一的位移表达式, 取如下形式

$$u_z(x, z, t) = w(x, t),\quad u_x(x, z, t) = -z\psi(x, t), \tag{5}$$

式中 $w(x, t)$ 表示中心线挠度, $\psi(x, t)$ 表示中心线法线的转角, 如图 1 所示.

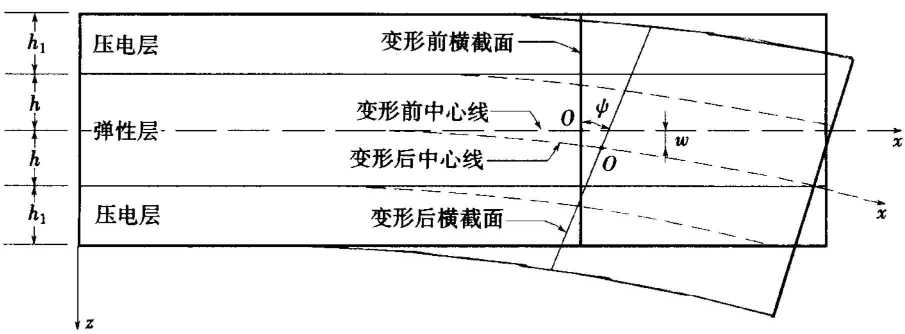

图 1 夹层梁位移假设图

一般的, 压电层电势 ϕ 由外加电压 $G(x, z, t)$ 和耦合电势 $\varphi(x, z, t)$ 共同组成. 考虑传感器极化方式及相应的激发与接收功能要求, 本文采用电势表达如下:

$$\begin{aligned}\phi_c(x, z, t) &= G(x, z, t) + \varphi(x, z, t) = \\ &\quad g(z)V_c(x, t) + f(z)\Phi_c(x, t) \qquad (c = \mathrm{A}, \mathrm{B}),\end{aligned} \tag{6}$$

式中, $V_c(x, t)$ 是外加电压 $G(x, z, t)$ 在表面电极中的分布(下标 A, B 分别表示上、下压电层), $g(z)$ 是该外加电压在厚度方向上的分布函数, 作线性分布假设: $\Phi_c(x, t)$ 是耦合电势 $\varphi(x, z, t)$ 在压电层中线的值, $f(z)$ 是该耦合电势在厚度方向上的分布函数. 对于压电层外表面电极

短路情况, 为满足Maxwell电荷方程, 弹性变形引起的耦合电势在厚度方向呈抛物线分布• 因此这里假设 $g(z)$ 和 $f(z)$ 分别为[13-14]:

$$g(z)=\begin{cases}-\dfrac{z+h}{h_1}, & z\subset \mathrm{A},\\ \dfrac{z-h}{h_1}, & z\subset \mathrm{B},\end{cases}\quad f(z)=\begin{cases}1-\left(\dfrac{z+h+h_1/2}{h_1/2}\right)^2, & z\subset \mathrm{A},\\ 1-\left(\dfrac{z-h-h_1/2}{h_1/2}\right)^2, & z\subset \mathrm{B}\bullet\end{cases}\tag{7}$$

将式(5)和(6)代入方程(2)和(3)就可计算压电层中的应力和电位移, 同样可计算弹性层中的应力, 于是可以按如下定义计算截面弯矩 M 和剪力 Q:

$$M_x=\int_{-h-h_1}^{h+h_1} z\sigma_x\,\mathrm{d}z=b_{12}\frac{\partial\psi}{\partial x}+b_{13}[\Phi_{\mathrm{A}}+(-1)^j\Phi_{\mathrm{B}}]+b_{14}[V_{\mathrm{A}}+(-1)^jV_{\mathrm{B}}],\tag{8}$$

$$Q_x=\int_{-h-h_1}^{h+h_1}\tau_{xz}\,\mathrm{d}z=$$
$$b_{21}\frac{\partial w}{\partial x}+b_{22}\psi+b_{23}\frac{\partial}{\partial x}[\Phi_{\mathrm{A}}+(-1)^j\Phi_{\mathrm{B}}]+b_{24}\frac{\partial}{\partial x}[V_{\mathrm{A}}+(-1)^jV_{\mathrm{B}}],\tag{9}$$

式中

$$\begin{cases}b_{12}=-\dfrac{2}{3}Eh^3-2c_{11}\dfrac{(h+h_1)^3-h^3}{3},\\ b_{13}=-e_{31}\left\{\dfrac{(h+h_1)^3-h^3}{3}+\dfrac{h+h_1/2}{2}[h^2-(h+h_1)^2]\right\}\dfrac{8}{h_1^2},\\ b_{14}=-e_{31}\dfrac{h^2-(h+h_1)^2}{2h_1},\quad b_{21}=-b_{22}=2k(Gh+c_{55}h_1),\\ b_{23}=\dfrac{2h_1}{3}e_{15},\quad b_{24}=\dfrac{h_1}{2}e_{15}\bullet\end{cases}\tag{10}$$

由于按式(5)计算的横向剪应变仅代表了梁的中性线的值, 在横截面上是一个常量, 为此引入剪切修正因子 k[15], 以考虑剪应变在横截面上非线性变化对剪力的修正•

3 弯曲元的梁方程

用 z 乘式(1)的第1式, 然后对它和式(1)的第2式分别沿梁的厚度积分, 利用式(5)、(6)及相关应力表达式, 得

$$-b_{21}\frac{\partial w}{\partial x}+\left(b_{12}\frac{\partial^2}{\partial x^2}-b_{22}-b_{42}\frac{\partial^2}{\partial t^2}\right)\psi+(b_{13}-b_{23})\frac{\partial}{\partial x}[\Phi_{\mathrm{A}}+(-1)^j\Phi_{\mathrm{B}}]=$$
$$m+(b_{24}-b_{14})\frac{\partial}{\partial x}[V_{\mathrm{A}}+(-1)^jV_{\mathrm{B}}],\tag{11}$$

$$-\left(b_{21}\frac{\partial^2}{\partial x^2}-b_{43}\frac{\partial^2}{\partial t^2}\right)w-b_{22}\frac{\partial\psi}{\partial x}-b_{23}\frac{\partial^2}{\partial x^2}[\Phi_{\mathrm{A}}+(-1)^j\Phi_{\mathrm{B}}]=$$
$$p+b_{24}\frac{\partial^2}{\partial x^2}[V_{\mathrm{A}}+(-1)^jV_{\mathrm{B}}],\tag{12}$$

式中 p 和 m 分别是梁单位长度上的力和力偶, 以及

$$b_{42}=-2\left[\frac{h^3}{3}\rho+\rho'\frac{(h+h_1)^3-h^3}{3}\right],\quad b_{43}=2(\rho h+\rho' h_1),\tag{13}$$

其中 ρ 和 ρ' 分别为弹性层和压电层的材料密度•

另外, 在梁的二维分析中, 压电层电位移需满足Maxwell方程的要求可由下面积分条件近似满足, 即

$$\int_{-h-h_1}^{-h}\left(\frac{\partial D_x}{\partial x}+\frac{\partial D_z}{\partial z}\right)\mathrm{d}z+\int_{h}^{h+h_1}\left(\frac{\partial D_x}{\partial x}+\frac{\partial D_z}{\partial z}\right)\mathrm{d}z=0. \tag{14}$$

将电位移 D_x 和 D_z 表达式代入式(14)得

$$2b_{31}\frac{\partial^2 w}{\partial x^2}+2b_{32}\frac{\partial\psi}{\partial x}+\left(b_{33}\frac{\partial^2}{\partial x^2}+b_{35}\right)[\Phi_A+(-1)^j\Phi_B]=$$
$$b_{34}\frac{\partial^2}{\partial x^2}[V_A+(-1)^jV_B], \tag{15}$$

式中

$$\begin{cases} b_{31}=ke_{15}h_1,\ b_{32}=-h_1(ke_{15}+e_{31}),\ b_{33}=-\dfrac{2h_1}{3}\varepsilon_{11}, \\ b_{34}=\dfrac{h_1}{2}\varepsilon_{11},\ b_{35}=\varepsilon_{33}\dfrac{8}{h_1}. \end{cases} \tag{16}$$

方程(11)、(12)和(15)就是压电夹层梁的控制方程. 当压电层反向极化时, 有 $j=1$, 此时表面电势反对称施加, 电学串联配置, 则有 $V_B=-V_A$, $\Phi_B=-\Phi_A$; 而压电层同向极化有 $j=2$, 此时表面电势对称施加, 电学并联配置, 则有 $V_B=V_A$, $\Phi_B=\Phi_A$. 因此, 方程(11)、(12)和(15)可进一步简化为(下式中 $\Phi=\Phi_A$, $V=V_A$)

$$-b_{21}\frac{\partial w}{\partial x}+\left(b_{12}\frac{\partial^2}{\partial x^2}-b_{22}-b_{42}\frac{\partial^2}{\partial t^2}\right)\psi+2(b_{13}-b_{23})\frac{\partial\Phi}{\partial x}=$$
$$m+2(b_{24}-b_{14})\frac{\partial V}{\partial x}, \tag{17}$$

$$-\left(b_{21}\frac{\partial^2}{\partial x^2}-b_{43}\frac{\partial^2}{\partial t^2}\right)w-b_{22}\frac{\partial\psi}{\partial x}-2b_{23}\frac{\partial^2\Phi}{\partial x^2}=p+2b_{24}\frac{\partial^2 V}{\partial x^2}, \tag{18}$$

$$b_{31}\frac{\partial^2 w}{\partial x^2}+b_{32}\frac{\partial\psi}{\partial x}+\left(b_{33}\frac{\partial^2}{\partial x^2}+b_{35}\right)\Phi=b_{34}\frac{\partial^2 V}{\partial x^2}. \tag{19}$$

4 简支梁算例

设 $m=0$, 将均布荷载 p 和常电压 V 展开成正弦级数形式:

$$\begin{cases} p(x,t)=\displaystyle\sum_{n=1}^{\infty}\left\{\frac{2p}{n\pi}[1-(-1)^n]\right\}\sin\left(\frac{n\pi}{l}x\right)e^{i\omega_n t}\triangleq\sum_{n=1}^{\infty}P_n\sin\left(\frac{n\pi}{l}x\right)e^{i\omega_n t}, \\ V(x,t)=\displaystyle\sum_{n=1}^{\infty}\left\{\frac{2V}{n\pi}[1-(-1)^n]\right\}\sin\left(\frac{n\pi}{l}x\right)e^{i\omega_n t}\triangleq\sum_{n=1}^{\infty}V_n\sin\left(\frac{n\pi}{l}x\right)e^{i\omega_n t}. \end{cases} \tag{20}$$

为满足两端简支边界条件 $w=0$, $\sigma_x=0$ 和 $\Phi=0$, 将挠度 w, 转角 ψ 和电势 Φ 展开成如下形式

$$\begin{Bmatrix} w(x,t) \\ \Phi(x,t) \end{Bmatrix}=\sum_{n=1}^{\infty}\begin{Bmatrix} W_n \\ \Phi_n \end{Bmatrix}\sin\left(\frac{n\pi}{l}x\right)e^{i\omega_n t},\quad \psi(x,t)=\sum_{n=1}^{\infty}\Psi_n\cos\left(\frac{n\pi}{l}x\right)e^{i\omega_n t}. \tag{21}$$

将式(20)和(21)代入式(17)~(19), 可得

$$\begin{bmatrix} a_{11} & a_{12} & a_{13} \\ a_{21} & a_{22} & a_{23} \\ a_{31} & a_{32} & a_{33} \end{bmatrix}\begin{Bmatrix} W_n \\ \Psi_n \\ \Phi_n \end{Bmatrix}=\begin{Bmatrix} -a_{14}V_n \\ P_n-a_{24}V_n \\ a_{34}V_n \end{Bmatrix}, \tag{22}$$

式中

$$\begin{cases} a_{11} = -b_{21}\dfrac{n\pi}{l},\ a_{12} = -b_{12}\left(\dfrac{n\pi}{l}\right)^2 - b_{22} + b_{42}\omega_n^2,\ a_{13} = 2(b_{13} - b_{23})\dfrac{n\pi}{l}, \\ a_{14} = -2(b_{24} - b_{14})\dfrac{n\pi}{l},\ a_{21} = b_{21}\left(\dfrac{n\pi}{l}\right)^2 - b_{43}\omega_n^2,\ a_{22} = b_{22}\dfrac{n\pi}{l}, \\ a_{23} = 2b_{23}\left(\dfrac{n\pi}{l}\right)^2,\ a_{24} = 2b_{24}\left(\dfrac{n\pi}{l}\right)^2,\ a_{31} = -b_{31}\left(\dfrac{n\pi}{l}\right)^2,\ a_{32} = -b_{32}\dfrac{n\pi}{l}, \\ a_{33} = -b_{33}\left(\dfrac{n\pi}{l}\right)^2 + b_{35},\ a_{34} = b_{34}\left(\dfrac{n\pi}{l}\right)^2. \end{cases} \quad (23)$$

对于外电极闭路时的自由振动分析, 只要令方程组(22)等式右边的荷载项为0即可• 图2给出了不同厚长比的前5阶频率比 ω_n/ω_n^*, 其中 ω_n^* 为二维精确解[16]• 由图2可见, 对不同夹层梁结构, 本简化模型精度很高, 对厚长比高达0.5的情况, 其误差仅在2%之内•

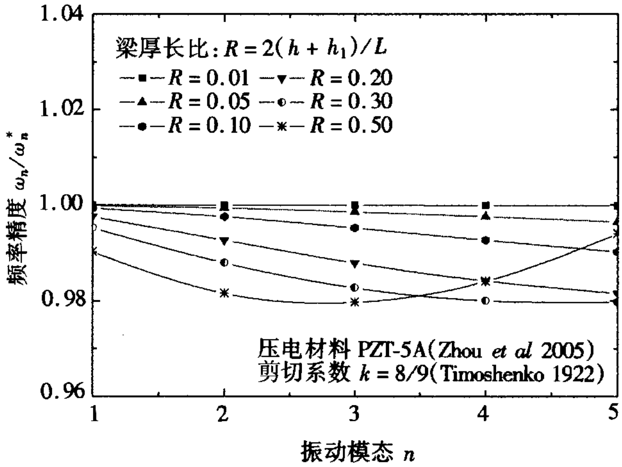

图2 弯曲元自由振动频率(外电极闭路)

5 结 论

本文在一阶剪切变形理论(FSDT)基础上, 对弯曲元压电层电势分布做了合理假设, 并引入合适的剪切修正因子 k 考虑横向剪应变的非线性分布, 建立了压电夹层梁的解析模型• 简支条件下弯曲元的自由振动分析表明, 本模型预测弯曲元较低模态频率有良好精度, 为压电弯曲元动力响应分析提供了良好的解析模型•

[参 考 文 献]

[1] Shirley D J, Hampton L D. Shear-wave measurements in laboratory sediments[J]. Journal of the Acoustic Society of America, 1978, **63**(2): 607-613.

[2] ZHOU Yan-guo, CHEN Yun-min. Influence of seismic cyclic loading history on small strain shear modulus of saturated sands[J]. Soil Dynamics and Earthquake Engineering, 2005, **25**(5): 341-353.

[3] Leong E C, Yeo S H, Rahardjo H. Measuring shear wave velocity using bender elements[J]. Geotechnical Testing Journal, 2005, **28**(5): 488-498.

[4] Viggiani G, Atkinson J H. Interpretation of bender element tests[J]. Geotechnique, 1995, **45**(1): 149-154.

[5] Arulnathan R, Boulanger R W, Riemer M F. Analysis of bender element tests[J]. Geotechnical Testing Journal, 1998, **21**(2): 120-131.
[6] Wood D Muir, Arroyo M, Greening P D. Source near-field effects and pulse tests in soil samples[J]. Geotechnique, 2003, **53**(3): 337-345.
[7] Lee J S, Santamarina J C. Bender elements: performance and signal interpretation[J]. Journal of Geotechnical and Geoenvironmental Engineering, ASCE, 2005, **131**(9): 1063-1070.
[8] Madabhusi-Raman P, Davalos J F. Static shear correction factor for laminated rectangular beams [J]. Composites Part B: Engineering, 1996, **27**(3): 285-293.
[9] Fernandes A, Pouget J. Analytical and numerical approaches to piezoelectric bimorph[J]. International Journal of Solids and Structures, 2003, **40**(17): 4331-4352.
[10] ZHOU Yan-guo, CHEN Yun-min, DING Hao-jiang. Analytical solutions to piezoelectric bimorphs based on improved FSDT beam model[J]. Smart Structures and Systems, 2005, **1**(3): 309-324.
[11] DING Hao-jiang, WANG Guo-qing, CHEN Wei-qiu. Green's functions for a two-phase infinite piezoelectric plane[J]. Proceedings of the Royal Society of London A, 1997, **453**(1966): 2241-2257.
[12] ZHOU Yan-guo, CHEN Yun-min, DING Hao-jiang. Analytical modelling and free vibration analysis of piezoelectric bimorphs[J]. Journal of Zhejiang University A Science, 2005, **6**(9): 938-944.
[13] Wang Q, Quek S T, Sun C T. et al. Analysis of piezoelectric coupled circular plate[J]. Smart Materials and Structures, 2001, **10**(2): 229-239.
[14] 丁皓江, 江爱民. 压电梁的多项式解(Ⅰ)——若干精确解[J]. 应用数学和力学, 2005, **26**(9): 1009-1022.
[15] Timoshenko S P. On the transverse vibrations of bars of uniform cross section[J]. Philosophical Magazine, Ser 6, 1922, **43**: 125-131.
[16] 周燕国. 土结构性的剪切波速表征及对动力特性的影响[D]. 博士论文. 杭州: 浙江大学, 2007.

Analytical Modeling of Sandwich Beam for Piezoelectric Bender Elements

ZHOU Yan-guo, CHEN Yun-min, DING Hao-jiang
(Key Laboratory of Soft Soils and Geoenvironmental Engineering, Ministry of Education, Zhejiang Unversity, Hangzhou 310027, P.R. China)

Abstract: Piezoelectric bender elements are widely used as electromechanical sensors and actuators. An analytical sandwich beam model for piezoelectric bender elements was developed based on the first-order shear deformation theory (FSDT), which assumes a single rotation angle for the whole cross-section and a quadratic distribution function for coupled electric potential in piezoelectric layers, and corrects the effect of transverse shear strain on the electric displacement integration. Free vibration analysis of simply-supported bender elements was carried out and the numerical results showed that solutions of the present model for various thickness-to-length ratios compare well with the exact two-dimensional solutions, which presents an efficient and accurate model for analyzing dynamic electromechanical responses of bender elements.

Key words: bender elements; piezoelectric; sandwich beam; shear correction factor; analytical model